

# Prediction-based Wind Turbine Operation for Active Participation in the Day-Ahead and Reserve Markets

N. Singh<sup>1,2</sup>, S. A. Hosseini<sup>3</sup>, N. Kayedpour<sup>1,2</sup>, J. D. M. De Koning<sup>1,4</sup>, Z. De Greve<sup>3</sup>,  
J. F. Toubeau<sup>3</sup>, F. Vallée<sup>3</sup>, G. Crevecoeur<sup>1,2</sup>, L. Vandeveldel<sup>1,2</sup>

<sup>1</sup>Department of Electromechanical, Systems and Metal Engineering, Ghent University, Ghent, Belgium

<sup>2</sup>FlandersMake@UGent - Core lab EEDT-DC, Flanders Make, Belgium

<sup>3</sup>Electrical Power Engineering Unit (EPEU), Power Systems and Markets Research Group, University of Mons, Mons, Belgium

<sup>4</sup>FlandersMake@UGent - Core lab EEDT-MP, Flanders Make, Belgium

**Abstract**—Electricity markets around the world are opening up to a greater contribution from wind power producers (WPPs). In this regard, WPPs are incentivised to participate in both energy and reserve market floors while being responsible for real-time deviations from their submitted bids. Therefore, despite uncertainties in wind speed and system frequency, effective control systems should be developed to enable WPPs to respond reliably concerning their committed day-ahead bids, as flexible conventional power plants do. However, designing a control system for WPP to regulate their capacity margin and output power as per the offered reserve bid is challenging, as a fast response with respect to the offered balancing service is required. This paper proposes an effective control system that allows WPP to regulate their set-points so as to provide the committed reserve power while considering the real-time wind variations. A machine-learning algorithm based on the Adaptive Neuro-Fuzzy Inference System (ANFIS) is used to predict the wind speed of the following instances, to be used as input to the control system. Several wind profiles are generated to simulate a practical case study, including real and predicted cases with varying levels of turbulence. Finally, the effectiveness of proposed control strategies on the WPP's profit is evaluated.

**Index Terms**—Wind energy, reserve market, control system, primary frequency control

## I. INTRODUCTION

Wind power generation across the world is increasing consistently. The year 2020 emerged as the best year in the history for wind power industry with 93 GW of new wind power installations and year-over-year growth of 53%, bringing the global cumulative wind power capacity to 743 GW [1]. The participation of wind energy in the ancillary services market is a matter of concern due to the inherent uncertainty and intermittent nature of wind power. The increasing participation of renewable energy in electricity markets tends to create a degradation of the frequency response. A possible solution to this problem and a way to increase WPP's profit, is increased participation of WPPs in the reserve market [2]. Studies have shown the feasibility of wind turbines in providing ancillary services such as primary reserve [3]. Also, the electricity markets around the world are increasingly offering shorter procurement periods for reserve power. These developments have incentivised a sustained research in this field. However, for

active participation in the joint day-ahead energy and reserve market (JERM) a fast response control system is required. There are several methods for the control of a direct-driven wind turbine [4]- [6]. A generator control method that uses interior permanent magnet synchronous generator (PMSG) controlled by a direct torque control scheme is presented in [7]. An improved direct torque control method for smooth power injection and short circuit protection is presented in [8]. These control strategies are widely used for variable-speed generation and for extracting the maximum power available in the wind. However, the control system proposed in this paper aims to explore the wind turbine control design that is capable of following not only the grid frequency but also the fast-varying wind speed in order to adjust the power output in real-time and maximise the WPP's profit. The proposed control system is validated with several tests for different control designs and wind profiles with different turbulence intensity levels (TIL). These wind profiles are then processed using a machine learning algorithm based on ANFIS to predict the wind speed data. The real and predicted wind profiles are then used in different case studies to analyse the control response. Finally, the results from the different operation strategies are evaluated focusing on the WPP's profit in the electricity market. The key contribution of this paper is proposing an advanced control strategy for reserve provision as well as evaluating the financial outcomes of such strategy for a WPP participating in JERM.

## II. MODEL

The simulation setup consists a wind turbine model in FAST, a generator model in MATLAB Simulink and a machine learning algorithm for wind speed prediction. These models are interconnected as a co-simulation with loop communications at each time-step of the simulation.

### A. Wind Turbine

The NREL 5 MW offshore wind turbine, developed in FAST, combines aerodynamic, hydrodynamic, structural and electrical properties of the wind turbine [9]. However, for this research, in order to retain flexibility over generator dynamics and the torque control system, the electrical part of the model

is replaced by a separate model in MATLAB Simulink. The main properties of the wind turbine are listed in Table I.

TABLE I  
WIND TURBINE PROPERTIES

Property	Specification
Power rating	5 MW
Rotor orientation & configuration	Upwind, 3 blades
Rotor and hub diameter	126 m and 3 m
Hub height	90 m
Cut-in, Rated and Cut-out wind speed	3.0 m/s, 11.4 m/s and 25.0 m/s

### B. Generator

The generator model used in this study is a PMSG with a rated power of 5 MW, rated speed of 12.1 rpm and a nominal efficiency of 93%. The equivalent diagram of the generator is presented in Fig. 1. The generator is modeled in the rotating (d,q) rotating reference frame. In Fig. 1,  $e_{PM,q}$  is the permanent magnet induced back-emf voltage, which is proportional to the rotor speed. The d and q equivalents also consist of an additional back-emf each proportional to the current in the other scheme due to the armature reaction effect.  $R_s$  and  $R_c$  respectively represent the copper losses in the stator winding and the iron losses. The values chosen for  $R_s$  and  $L_q$  are 98.5 mΩ and 5.86 mH, respectively.

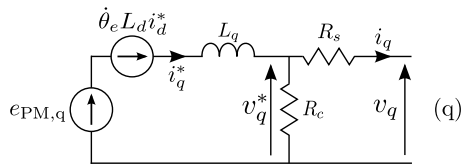


Fig. 1. Equivalent diagram of a PMSG in the rotating reference frame

### C. Wind profile design and prediction

TurbSim, an open source tool is used to generate the primary wind field used in the simulations. The IEC Kaimal turbulence model is used to generate several wind profiles with different TIL. This study also uses a machine-learning algorithm based on ANFIS to predict the time-series wind speed data. It involves building a fuzzy-based neural network that learns historical wind information and uses it to observe future sequences [10]. Fortunately, high-quality offshore wind profile measurements are now possible using LIDAR technology, which provides a full 3D spatial mapping of the wind field at multiple heights [11]. The time-series prediction represents a model that uses past values to predict future values. Historical time-stamped wind data are entered into the ANFIS structure as inputs, and the predicted future data will be expected as an output. In general, a non-linear autoregressive model represents this prediction, obtained by the following equation:

$$x(k+t) = f[x(k), x(k-1), x(k-2), \dots, x(k-n-1)] \quad (1)$$

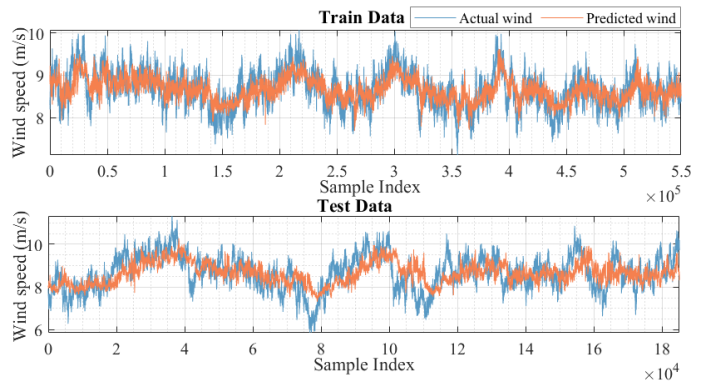


Fig. 2. Train and test datasets for ANFIS model (60-min).

where, the function  $f$  can find the nonlinear relationship of past, present, and future values of the  $x$  over a set period  $t$ . In this study, the FIS structure is generated using fuzzy c-means clustering. The Gaussian distribution is considered for membership functions. For training the network, 750,000 data samples are obtained from an hour wind simulation, in which 70% of the data points are randomly chosen for training the network and 30% of the data points are used for test and validation. The training and testing results are shown in Fig. 2.

### III. CONTROL AND OPERATION STRATEGY

In what follows, the control system and different operation strategies will be described. The operation strategies determine the power set-point, which is tracked by the control system.

#### A. Control system

The control system developed for this research aims to track the maximum power point as well as time-varying deloaded power set-points, in order to track the grid frequency and wind speed as per the bids offered in the energy and reserve markets. The controller at its base is a field oriented control system where the direct current component is regulated to zero and the quadrature current is in proportion with the torque. The PI control scheme is presented in Fig. 3. The PI controller takes as input, the difference between the reference power and the actual power output from the generator at each time step. The PI controller generates a torque control signal in the form of quadrature current  $i_q$  such that the error is minimised.

The control design is based on the 200 mHz symmetrical ancillary service as defined in [12]. Fig. 4 shows a graphical representation of this service. The frequency based time-varying reference power  $P_{ref}$  is defined in (2). For a WPP participating in the reserve market with a bid of  $P_{RM}$  must maintain  $P_{ref}$  as the sum of base power  $P_{base}$  and frequency based power  $P_f(t)$ .  $P_f(t)$  is a time varying quantity proportional to the grid frequency.  $P_f(t)$  varies linearly between  $-P_{RM}$  and  $+P_{RM}$  for the grid frequency of 50.2 Hz and 49.8 Hz respectively. A controller following such service must be capable to follow these downwards and upwards ramps within the specified time. However, for the research presented in this paper only the frequency range within 49.8 Hz - 50 Hz

is considered, as this range requires power up-regulation which is a more complex control implementation.

$$P_{\text{ref}} = P_{\text{base}} + P_f(t) \quad (2)$$

For the operation strategy that uses wind speed to determine the maximum available power, a lookup table based on the power curve of the wind turbine is used. The power curve of the wind turbine is presented in Fig. 5. For the performance analysis of the controller, a test as presented in Fig. 6 is simulated. Two cases with a highly turbulent wind speed are simulated. The grid frequency in the two cases is on the margins of the 200 mHz symmetrical service, i.e., 49.8 Hz and 50.2 Hz respectively. A 5 MW wind turbine offering 1 MW of FCR for such a service will need to maintain a base power of 4 MW and a ramp-up and ramp-down of the power output within the range of 3-5 MW, based on the grid frequency. The controller shows an efficient performance and the maximum error in both these cases does not exceed 1%.

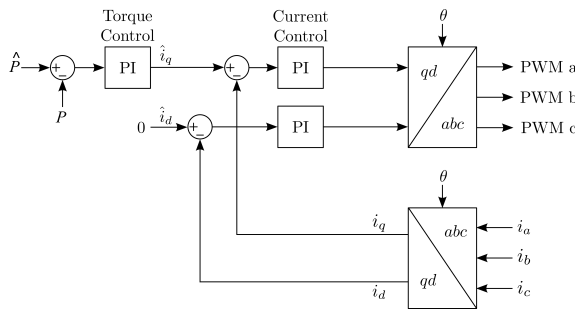


Fig. 3. Field oriented control of PMSG

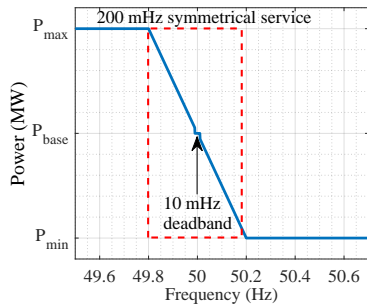


Fig. 4. Control for a 200 mHz service

### B. Operation Strategy

Our optimal decisions framework, developed in [13], is considered for the participation of the WPP in JERM. The market incentives in the day-ahead market for energy and reserve floors are 33 €/MWh and 34 €/MW, respectively. Also, the market rate regarding energy imbalance settlement (EIS) for deficit and surplus of generations are, 35 €/MWh and 30 €/MWh, respectively. Finally, the balancing stage penalty rate regarding the unavailability of the offered FCR in real-time is 45 €/MW. The employed decision tool considers wind

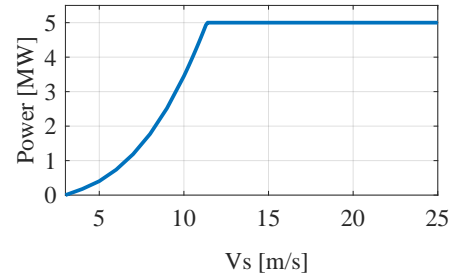


Fig. 5. Power curve of the 5 MW offshore wind turbine

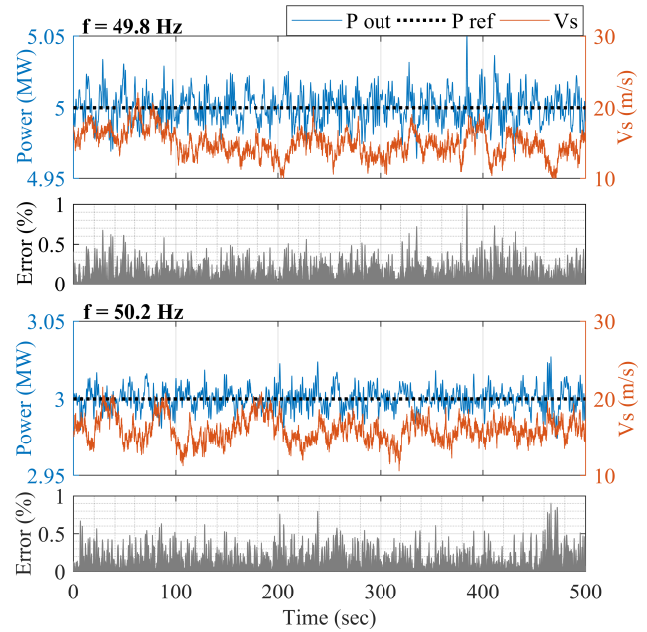


Fig. 6. Controller performance

uncertainty and market incentives to return the optimal share of power assigned to energy and reserve market floors, thereby maximizing the WPP's profit. In this regard, the optimal decisions concerning the day-ahead energy  $P_{EM}$  and reserve bids  $P_{RM}$  are respectively, 0.5 MWh and 1.78 MW. Hence, the fixed day-ahead revenue of WPP in the day-ahead energy and reserve market is € 16.49 and € 60.72, respectively. Additionally, the employed decision tool considers financial compensations regarding real-time energy and reserve power bids deviations.

In Fig. 7, three operation strategies are introduced to evaluate the effectiveness of the proposed control system. Notably, the evaluation is performed based on wind speed profiles with medium and high TIL (5% and 10%, respectively), for a duration of 1 hour. At first, an illustrative case, using two wind profiles, is presented to observe the advantages of the proposed method.

1) *Operation strategy 1*: Operation Strategy 1 (OS-1) uses an advanced control strategy where the reference power of the control system is not only based on system frequency

and the day-ahead optimal bids but also based on the actual wind speed. This ideal strategy assumes that the real-time wind speed is known. Therefore, the control is designed such that if the maximum available power  $P_{\max}$  in the wind is greater than  $P_{RM}$ , the reference power  $P_{ref}$  is equivalent to  $P_{\max} - P_{RM}$ . Whereas, if  $P_{\max}$  is less than  $P_{RM}$ ,  $P_{ref}$  is maintained at 0. In this way, the reserve market bid is given priority.

2) *Operation strategy 2*: Operation Strategy 2 (OS-2) is a naive strategy which merely employs a static reference power along with system frequency to adjust the wind turbine's output so as to maintain the scheduled reserve capacity margin. The controller is designed to linearly operate to generate  $P_{ref}$  equal to set-points 2.28 MW and 0.5 MW for the two frequency cases of 49.8 Hz and 50 Hz, respectively. The wind dynamics are disregarded in this strategy. These fixed set-points correspond to the power quantities regarding the energy and reserve markets obtained by the optimal decision tool.

3) *Operation strategy 3*: Operation Strategy 3 (OS-3) is an operable implementation of the advanced variable reference control strategy based on a predicted wind speed and the day-ahead optimal bids. Since the actual wind speed for the next time-step is unknown to the control system, in order to implement OS-1, a prediction of wind speed at the next time-step is required. Therefore, in OS-3, a prediction model cfr. § II-C, is utilized to predict the wind speed.  $P_{ref}$ , in this strategy is determined using both, real wind  $V_{real}$  and predicted wind  $V_{pred}$  values such that the upper bound of  $P_{ref}$  is limited by  $V_{real}$  based  $P_{\max}$ . To implement this,  $V_{pred}$  is compared to  $V_{real}$  at each time-step. If  $V_{pred}$  is greater than  $V_{real}$ , then  $P_{ref}$  is based on  $V_{real}$ . Else,  $P_{ref}$  is based on  $V_{pred}$ .

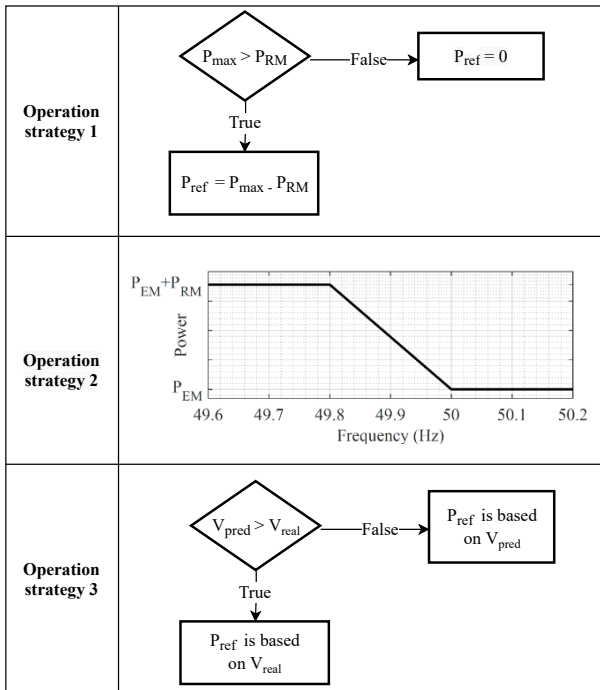


Fig. 7. Operation strategies

## IV. RESULTS

### A. Illustrative example

Fig. 8 shows the real-time power submitted to the energy-only market (blue lines). In this case, the system frequency during the 1-hour dynamical ex-post simulation is set to 50 Hz, thus the reserve capacity is not activated. On the other hand, the red lines show the wind turbine output power for a system frequency below 49.8 Hz. In this case, the output power is the summation of the activated reserve capacity and the power submitted to the energy market. Importantly, the area between these 2 curves shows the power that is potentially kept as reserve capacity. Fig. 8 (a) - (b) shows the harvested wind power using the ideal strategy, OS-1, for wind profiles with both 5% and 10% TIL. The average output power to the energy market for 5% and 10% TIL is respectively, 0.438 MW and 0.545 MW. Moreover, the wind turbine's mean output power for full reserve power activation is 2.215 MW and 2.261 MW, respectively. This can be interpreted as leaving a capacity margin of 1.778 MW and 1.716 MW regarding the 5% and 10% TIL. With this approach, WPP can stay around its submitted day-ahead energy and reserve bids in real-time. The naive strategy, OS-2, submits an average power of 0.5 MW to the energy market regardless of the TIL. Also, the total average submitted power to the network when the reserve is fully activated for TIL 5% and 10% is, respectively, 2.116 MW and 2.010 MW. Thus, the maintained mean capacity margin is 1.616 MW and 1.510 MW for the medium and high TILs, respectively. Note that, as seen in Fig. 8 (c) - (d), while the average area between the two curves is still fairly close to  $P_{RM}$ , there are several periods with power deficits concerning the scheduled reserve power. On the other hand, as seen in Fig. 8 (e), the total power submitted to the energy market using the proposed strategy, OS-3, is 0.418 MW and 0.447 MW, for 5% and 10% TIL, respectively. Also, as shown Fig. 8 (f), for a system frequency less than 49.8 Hz, OS-3, returns a mean output power of 2.108 MW and 2.033 MW for TIL of 5% and 10%, respectively. It means that OS-3, on average, is able to keep a reserve capacity of 1.5861 MW and 1.6896 MW concerning the wind profiles with 5% and 10% TIL, respectively. Remarkably, while the average reserve power in OS-3 is lower than the naive strategy, OS-2, the periods with a high deficit of reserve power availability are lower than OS-2 (this is seen in Fig. 8 (c) - (d) and is further verified in the next subsection by comparing the real-time market penalties). Accordingly, the average reserve capacity margin kept in real-time, and well as the average submitted power to the energy market is not only close to the day-ahead bids, but also similar to the one obtained by the ideal strategy, OS-1 as compared to OS-2.

### B. Out-of-sample analysis

While observing the overall effectiveness of the proposed control strategy using the illustrative example, an out-of-sample analysis is performed (see Table II). In this way, we are able to correctly evaluate the advantages of the proposed

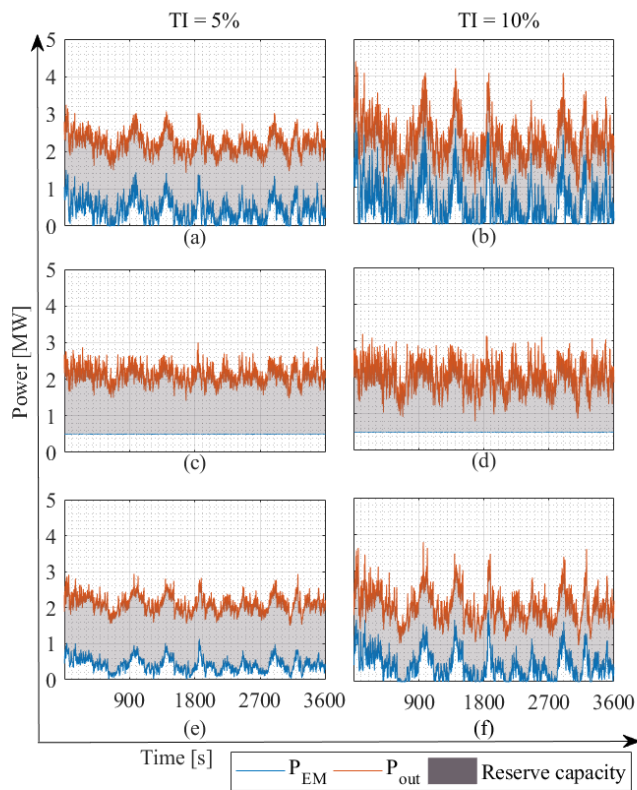


Fig. 8. Power outputs and reserve margin

control strategy with respect to the expected in-sample results (obtained by the bidding model as reported in the last column of Table II) and other strategies. The expected market revenue streams, i.e., contribution regarding EIS for deficit  $\Pi^{E-}$  and surplus  $\Pi^{E+}$  of generation, as well as the balancing stage penalty  $\Pi^{R-}$ , will be compared to three operation strategies in order to evaluate their performance. As seen in Table II, the penalty paid by WPP using the ideal control strategy, OS-1, is close to the expected revenue streams. Specifically, in this case, the total revenue of the WPP for 5% and 10% TILs are, respectively, € 72.91 and € 72.48 (which is close to the corresponding expected value € 74.49). On the other hand, the naive model, OS-2, is unable to provide the reserve power for many periods, thus paying a high penalty at the balancing stage (i.e., € -9.1028 and € -14.69 regarding 5% and 10% TIL, respectively). Therefore, the overall revenue is greatly lower than the expected values (€ 68.10 and € 62.52 respectively, for TIL of 10% and 5%). Finally, it is seen that the total revenue obtained by the practical realization of the ideal strategy, OS-3, acquires a higher profit than the OS-2 (i.e., € 69.591 and € 65.702 for 5% and 10% TILs). That is since the penalty paid by WPP due to the inability to activate the committed reserve is lower than OS-2.

## V. CONCLUSION

An operation strategy is developed that allows WPPs to participate in the JERM. The proposed control strategy not

TABLE II  
REVENUE (€)

	OS-1		OS-2		OS-3		Expected
TI	5%	10%	5%	10%	5%	10%	-
$\Pi^{E+}$	0	2.02	0	0	0	0.2	3.69
$\Pi^{E-}$	-2.17	-0.78	0	0	-2.86	-2.08	-5.85
$\Pi^{R-}$	-2.13	-5.97	-9.1028	-14.69	-4.759	-9.628	-0.57
$\Pi$	72.91	72.48	68.10	62.52	69.591	65.702	74.49

only takes system frequency and scheduled bids as input but also predicts the wind speed of the next time-step to properly adjust the reference power, thus providing the reserve power. The controller is validated with an efficient performance for several cases with varying level of TILs. The effectiveness of the proposed control strategy is also validated ex-post, based on the optimal WPP bidding decisions.

## ACKNOWLEDGMENT

This work is supported by the BEOWIND project, funded by the Energy Transition Fund of the Belgian government.

## REFERENCES

- [1] "Global Wind Report 2021 - Global Wind Energy Council", Global Wind Energy Council, 2021. [Online]. Available: <https://gwec.net/global-wind-report-2021/>.
- [2] Hosseini, S. A.; Toubeau, J.-F.; Singh, N.; De Kooning, J. D. M.; Kayedpour, N.; Crevecoeur, G.; De Grève, Z.; Vallée, ; Vandeveld, L.: 'Impact of fast wind fluctuations on the profit of a wind power producer jointly trading in energy and reserve market', IET Conference Proceedings, 2021, DOI: 10.1049/icp.2021.1386.
- [3] N. Singh, J. D. M. De Kooning and L. Vandeveld, "Simulation of the Primary Frequency Control Pre-Qualification Test for a 5MW Wind Turbine," 2020 IEEE/PES Transmission and Distribution Conference and Exposition (T&D), 2020, doi: 10.1109/TD39804.2020.9299921.
- [4] S. Li, T. A. Haskew, R. P. Swatloski and W. Gathings, "Optimal and Direct-Current Vector Control of Direct-Driven PMSG Wind Turbines," in IEEE Transactions on Power Electronics, May 2012.
- [5] X. Zeng, T. Liu, S. Wang, Y. Dong and Z. Chen, "Comprehensive Coordinated Control Strategy of PMSG-Based Wind Turbine for Providing Frequency Regulation Services," in IEEE Access, 2019.
- [6] Z. Zhang, Y. Zhao, W. Qiao and L. Qu, "A Discrete-Time Direct Torque Control for Direct-Drive PMSG-Based Wind Energy Conversion Systems," in IEEE Transactions on Industry Applications. 2015.
- [7] Y. Inoue, S. Morimoto and M. Sanada, "Control method for direct torque controlled PMSG in wind power generation system," 2009 IEEE International Electric Machines and Drives Conference, 2009, doi: 10.1109/IEMDC.2009.5075360.
- [8] Abdolghani, Nazanin, Jafar Milimonfared and Gevork Babamalek Gharehpetian. "A Direct Torque Control Method for CSC Based PMSG Wind Energy Conversion Systems." Renewable energy & power quality journal (2012).
- [9] J. Jonkman, S. Butterfield, W. Musial, and G. Scott, "Definition of a 5-MW Reference Wind Turbine for Offshore System Development," 2009.
- [10] Khosravi, Ali, Luiz Machado, and R. O. Nunes. "Time-series prediction of wind speed using machine learning algorithms: A case study Osorio wind farm, Brazil." Applied Energy (2018).
- [11] Mikkelsen, Torben, et al. "A spinner-integrated wind lidar for enhanced wind turbine control." Wind Energy (2013).
- [12] Elia, "General Framework for Frequency Containment Reserve Service by Non-CIPU resources".
- [13] Seyyed Ahmad Hosseini, Jean-François Toubeau, Zacharie De Grève, François Vallée, "An advanced day-ahead bidding strategy for wind power producers considering confidence level on the real-time reserve provision, Applied Energy, <https://doi.org/10.1016/j.apenergy.2020.115973>.